LAWRENCE
LIVERMORE
NATIONAL
LABORATORY

LLNL-CONF-418042

DETAILED CHEMICAL KINETIC MODELING OF ISO-OCTANE SI-HCCI TRANSITION

M. A. Havstad, S. M. Aceves, M. J. McNenly, W. T. Piggott, K. D. Edwards, R. M. Wagner, C. S. Daw, C. E. A. Finney

October 14, 2009

Society of Automotive Engineers 2010 world conference
detroit, MI, United States
April 13, 2010 through April 15, 2010

Disclaimer

10PFL-0840

Detailed Chemical Kinetic Modeling of Iso-octane SI-HCCI Transition

Mark A. Havstad, Salvador M. Aceves, Matthew J. McNenly, William T. Piggott
Lawrence Livermore National Laboratory

K. Dean Edwards, Robert M. Wagner, C. Stuart Daw, Charles E. A. Finney
Oak Ridge National Laboratory

ABSTRACT

We describe a CHEMKIN-based multi-zone model that simulates the expected combustion variations in a single-cylinder engine fueled with iso-octane as the engine transitions from spark-ignited (SI) combustion to homogenous charge compression ignition (HCCI) combustion. The model includes a 63-species reaction mechanism and mass and energy balances for the cylinder and the exhaust flow. For this study we assumed that the SI-to-HCCI transition is implemented by means of increasing the internal exhaust gas recirculation (EGR) at constant engine speed. This transition scenario is consistent with that implemented in previously reported experimental measurements on an experimental engine equipped with variable valve actuation. We find that the model captures many of the important experimental trends, including stable SI combustion at low EGR (~0.10), a transition to highly unstable combustion at intermediate EGR, and finally stable HCCI combustion at very high EGR (~0.75). Remaining differences between the predicted and experimental instability patterns indicate that there is further room for model improvement.

INTRODUCTION

An improvement in the fuel efficiency of gasoline engines is necessary to realize a significant reduction in U.S. energy usage. Homogeneous charge compression ignition (HCCI) in internal combustion engines is of considerable interest because of the potential reductions in flame temperature and nitrogen oxide (NO_x) emissions as well as potential fuel economy improvements resulting from un-throttled operation, faster heat release, and reduced heat transfer losses. Unfortunately for many transportation applications, HCCI may not be possible or practical under the full range of speed and load conditions. Thus, the most important technical developments needed to achieve wide-spread HCCI utilization are expansion of the operational range and the ability to switch between HCCI and traditional propagating flame (e.g., spark ignition, SI) combustion as power and speed change. Recent publications and presentations have begun to address the control issues related to such combustion mode transitions [1-4] with limited focus on the fundamental nature of the transition dynamics associated with switching from SI to HCCI combustion [5-6]. The development of both combustion-mode switching and stabilization technologies requires that the fundamental nature of the transition be well understood, especially in the context of realistic engine conditions.

The goal of the current work is to develop a pragmatically detailed model capable of simulating the complex dynamic behavior observed during SI-HCCI transitions. Insight gained from this model into the mechanisms driving the inherent combustion instabilities can then be used to direct efforts to develop real-time diagnostics and controls for smoothing the SI-HCCI transition and stabilizing spark-assisted HCCI.

Current models range in detail and complexity from one-zone, single-burn equation models to full CFD models with many thousands of zones and hundreds of species [7-9]. All of these have demonstrated utility. Lumped models have applicability to simplified engine modeling based on heat transfer and flame speed correlations. However, these correlations typically do not capture the substantial cycle-to-cycle variations present in SI-HCCI transitions. High-resolution fluid mechanics linked with chemical kinetics in KIVA [10] or other codes enables high-fidelity engine modeling. However, long running times typically preclude KIVA analysis of successive engine cycles which is necessary for SI-HCCI transition modeling. Modeling of marginal flame propagation in high-EGR SI operation is also a considerable challenge for KIVA SI-HCCI modeling.

In order to reach a compromise between the computational expense of KIVA-like models and the lack of resolution of single-zone models, we constructed a multi-zone combustion model that would allow us to investigate the simultaneous roles of chemical kinetics and fluid mechanics on the cycle-to-cycle dynamics. Multi-zone kinetics has the potential of capturing the whole range of combustion events: robust SI flame propagation, weak SI flames, and HCCI autoignition – all within a reasonable computational time (minutes per engine cycle) that enables analysis of multiple consecutive engine cycles necessary for transition modeling. While the multi-zone model does require tuning of the mixing rates between zones, satisfactory results are demonstrated for a variety of conditions after tuning for robust SI flame propagation. No tuning is necessary for kinetics-controlled HCCI combustion, the mixing rates are effectively set to zero.

In the work presented here, we apply a 12 zones model for the combustion chamber and a reduced isooctane chemical kinetic mechanism where 63 species participate kinetically and 152 are treated as quasi-steady species [11], with a total of 964 explicitly solved kinetic reactions. By incorporating recent advances in the numerics of the non-linear iteration [12], the model is capable of simulating – in a reasonable amount of time – we have been able to simulate a sufficient number of engine cycles to compare predicted behavior to experimental observations over a range of conditions.

EXPERIMENTAL PROCEDURE AND OBSERVATIONS

The experimental observations discussed here were made using a 0.5-L single-cylinder AVL research engine with 11.34:1 compression ratio. The engine cylinder geometry is summarized in Table 1. This engine has two intake valves and one exhaust valve and is equipped with a full-authority hydraulic variable valve actuation (VVA) system. Only a single intake valve was used in this study to promote swirl and mixing. HCCI operation was achieved by varying the valve timing and lift to increase internal EGR through negative valve overlap. Rapid transitions between SI and HCCI operation were found to produce significant combustion variability and occasional engine stall. To explore the dynamics of the SI-HCCI transition in greater detail, a series of experiments were conducted by incrementally varying the valve settings and allowing the engine to reach steady state. Table 2 provides valve settings and internal EGR levels (estimated using a WAVE® model of the engine) for a selection of operating points mentioned in the discussion below.

The fuel (iso-octane) was delivered by an intake mounted port fuel injector. Engine speed was maintained constant using an absorbing/motoring dynamometer. Nominal operating conditions corresponded to 1600 rpm and 3.4 bar indicated mean effective pressure (IMEP). Throughout the EGR range, spark timing was held fixed at 25°BTDC and coolant temperature maintained at 90°C. At EGR levels typically in excess of 55%, full HCCI operation was achieved, and the spark could be turned off with no impact on combustion. Fueling rate was maintained constant, and intake throttling used to maintain a stoichiometric air-fuel ratio. Typically, the throttle was wide open for pure HCCI operation.

Table 1 Engine geometry and operating parameters

Speed	1600 rpm
Bore	0.0902 m
Stroke	0.0900 m
Compression Ratio	11.34
Connecting Rod Length	0.1507 m

In-cylinder pressure measurements were recorded at resolution of 0.5 crank-angle-degrees for each internal EGR level. To minimize non-combustion artifacts, all engine feedback controllers were shut off, and the engine was operated in open-loop mode except for the dynamometer speed controller and coolant temperature controller. Measurements at each specific EGR level typically included 3000 consecutive engine cycles. Standard exhaust gas instrumentation was used including steady-state measurements of CO, CO_2, HC, NO_x, and O_2 concentrations in the raw engine-out exhaust. The normal procedure following each incremental EGR adjustment was to allow the engine to run several minutes to reach 'steady-state' (for oscillatory combustion states, this meant that the behavior became statistically stationary or consistent over time). Data was not acquired during transitions between EGR levels. Following this run-out period, in-cylinder pressure and standard engine temperature and exhaust gas analyses were recorded for the required time. Cycle-resolved heat release rate, integrated heat release (HR), and IMEP were calculated from the measured in-cylinder pressure measurements following standard procedures in the literature [13].

Table 2 Valve timing and lift parameters for discussed cases

Case	EVO, ^{o}ATDC	EVC, ^{o}ATDC	EV Lift, mm	IVO, ^{o}ATDC	IVC, ^{o}ATDC	IV Lift, mm	Estimated EGR Level
Baseline SI	184	336	6.0	374	-186	6.0	10%
A (SI)	181	308	5.3	398	-180	6.1	25%
B	179	289	4.9	414	-176	6.2	37%
C	178	282	4.7	420	-174	6.2	41%
D	177	275	4.5	423	-173	6.3	45%
E	175	251	4.0	446	-168	6.4	55%

F (HCCI)	172	230	3.5	463	-166	6.5	75%

The overall dynamic behavior observed in the iso-octane experiments is very similar to previously reported observations using indolene and an 85/15 ethanol/indolene (E85) blend [14,15] although the engine exhibited more dynamic noise when fueled with iso-octane or E85. This similarity suggests that the basic kinetic pathways for HCCI are similar for these fuels. As detailed elsewhere [6,14-19], using a variety of analysis techniques, we have developed an understanding of how the combustion behavior changes as internal EGR is increased to transition from SI to HCCI. We summarize these observations below. Through the development of this detailed kinetic model, we hope to better understand the underlying causes of this behavior and learn better ways to stabilize HCCI combustion.

Figures 1-3 demonstrate the complexity of the combustion instabilities that develop during the SI-HCCI transition. Data shown in each of these figures correspond to the selected cases A-F detailed in Table 2. Figure 1 presents first-return maps of cycle-integrated heat release that allow one to assess the level of influence past events have upon current events. Points in Figure 1 below the diagonal signify heat release less than that of the prior cycle and points above the diagonal signify heat release greater than that of the prior cycle. Figure 2 presents a selection of short time series segments of cycle-integrated heat release that provides a different view of the combustion instabilities and demonstrates some of the repeating patterns of behavior. Different lines in Figure 2 refer to different starting points within the set of 3000 sequential cycles stored from each EGR setting. Finally, Figure 3 presents histograms of the cycle-integrated heat release for each case.

At lower internal EGR levels (cases A and B), communication between cycles is limited and dilution levels are too low to have significant impact on flame speed. As a result, combustion is dominated by SI and is stable as indicated by the tight clustering of points about a single value on the return maps in Figures 1a-b. Combustion variability is small as indicated by the low COV in IMEP (2-4%) and appears stochastic in nature as indicated by the Gaussian distribution shown in Figures 3a-b. At high EGR levels (case F), dilution is too high to support a propagating flame and combustion is dominated by HCCI. Despite the greater opportunity for communication between cycles, combustion is stable with little cycle-to-cycle variability and a COV in IMEP of 2.5%.

At intermediate EGR levels (cases C-E), behavior becomes much more complex as SI and HCCI compete with one another, even occurring together during the same cycle. Combustion mode switches between SI, HCCI, and spark-assisted HCCI from one cycle to the next as conditions within the cylinder dictate. Complex, recurring patterns of behavior are observed as combustion becomes stabilized or destabilized due to small changes in the temperature and composition of the residual gases. The complexity and deterministic nature of the behavior can be seen in the return maps in Figures 1c-e. It has been observed that cycles that fall along the lower portion of the diagonal in these plots undergo incomplete SI combustion. Such cycles are typically followed by incomplete HCCI events that fall above the diagonal. These events are then followed by cycles that fall below or along the upper portion of the diagonal and that experience spark-assisted HCCI in which a flame is initiated by the spark and propagates across the cylinder until conditions are favorable for the remaining end gases to ignite. Spark-assisted HCCI combustion will often become stable for several consecutive cycles when SI and HCCI are in relative proportions. Examples of this behavior can be seen in some of the time series segments in Figure 2d-e where heat release remains relatively constant for several consecutive cycles. However, conditions will eventually develop that favor one mode over the other. This destabilizes the system resulting in rapid combustion mode switching (often following recurring patterns as seen in Figure 2d and described above) until the system can again reach equilibrium. The modeling is intended to

gain insight into the patterns of of combustion instability and the role of the composition and temperature of the residual gases.

There are conditions (such as in case E) where steady-state operation is difficult because dilution is too high to support SI combustion but not high enough to support full transition to HCCI. Misfire becomes more prevalent (as seen in the time series segments in Figure 2e and the dominance of the zero-heat-release bin in Figure 3e) cooling the engine and often leading to engine stall.

Spark-assisted HCCI produces NO_x emissions similar to HCCI but with lower pressure rise rates making it a promising approach for operating at higher loads than can be achieved with pure HCCI [14]. However, a better understanding of the fundamental causes of the combustion instabilities is needed in order to develop better controls to further stabilize combustion.

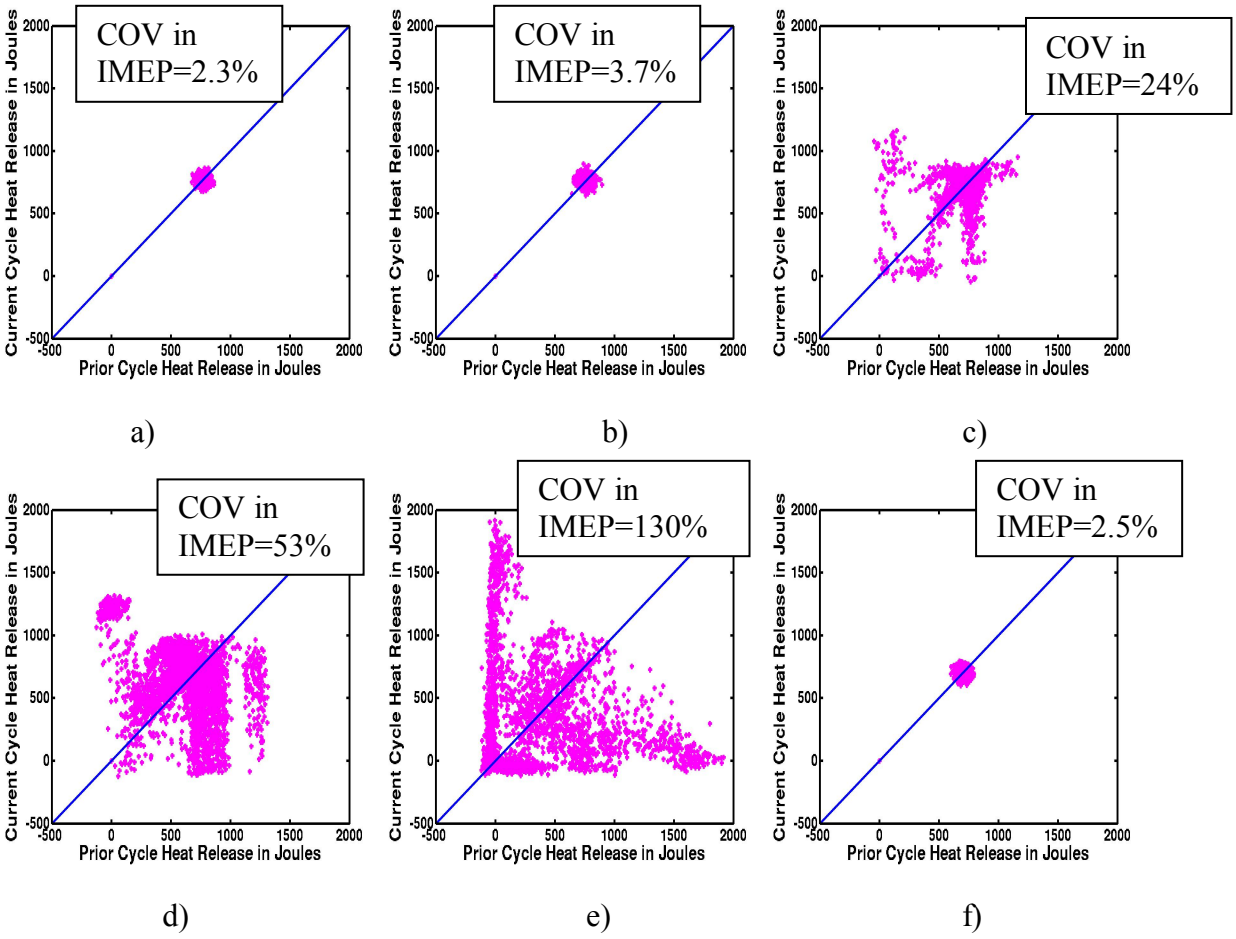

Figure 1 Experimental first-return maps of integrated heat release reveal the complex, deterministic dynamics observed during steady-state operation along the SI-HCCI transition pathway. Plots a) - f) correspond to cases A-F in Table 2.

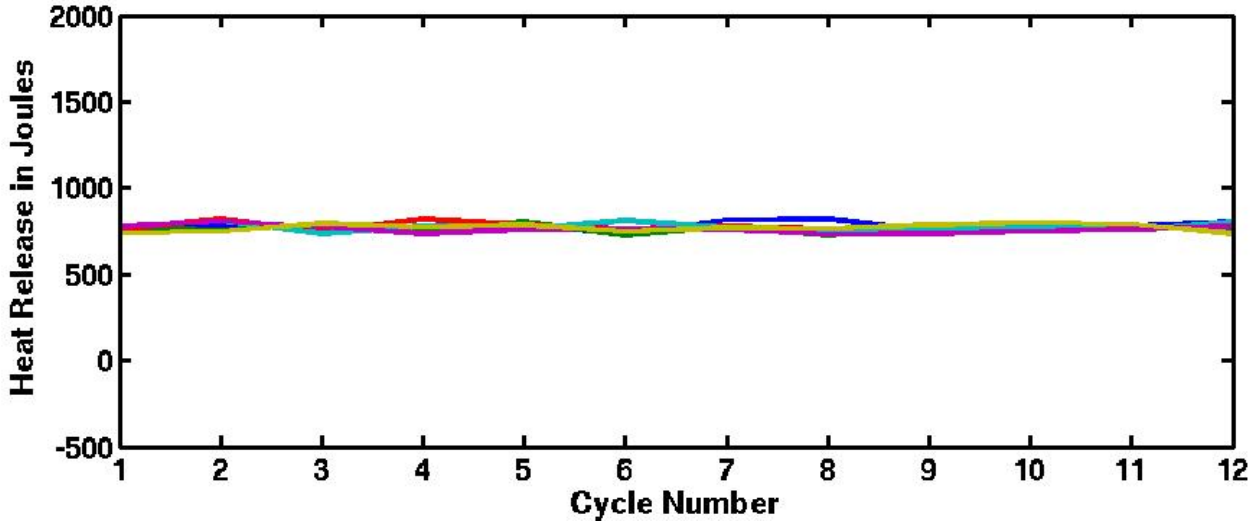
Heat Release in Joules
2000
1500
1000
500
0
-500
1
2
3
4
5
6
7
8
9
10
11
12
Cycle Number

a)

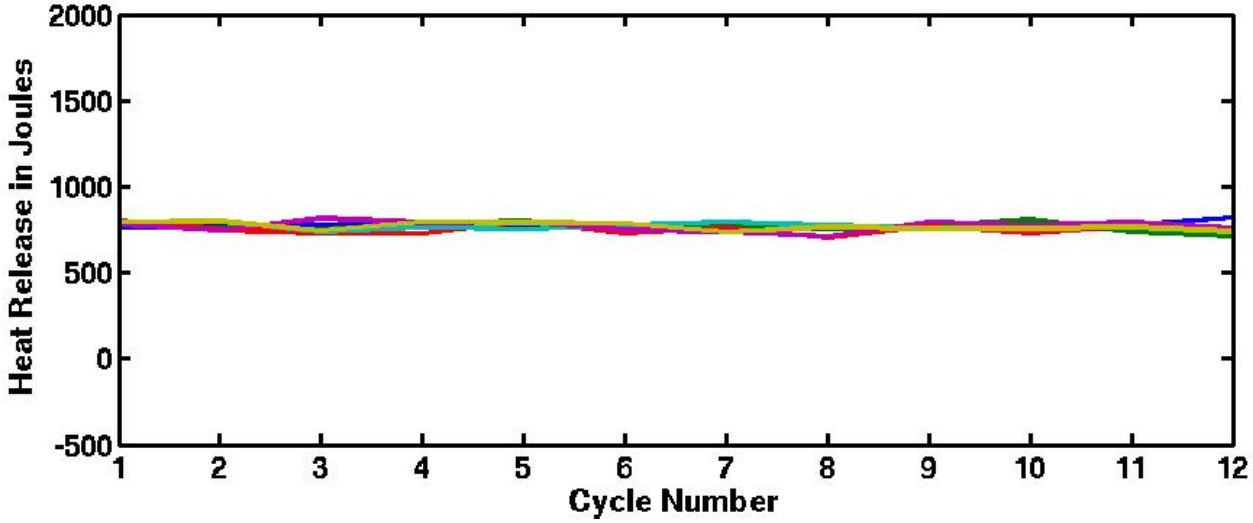
Heat Release in Joules
2000
1500
1000
500
0
-500
1
2
3
4
5
6
7
8
9
10
11
12
Cycle Number

b)

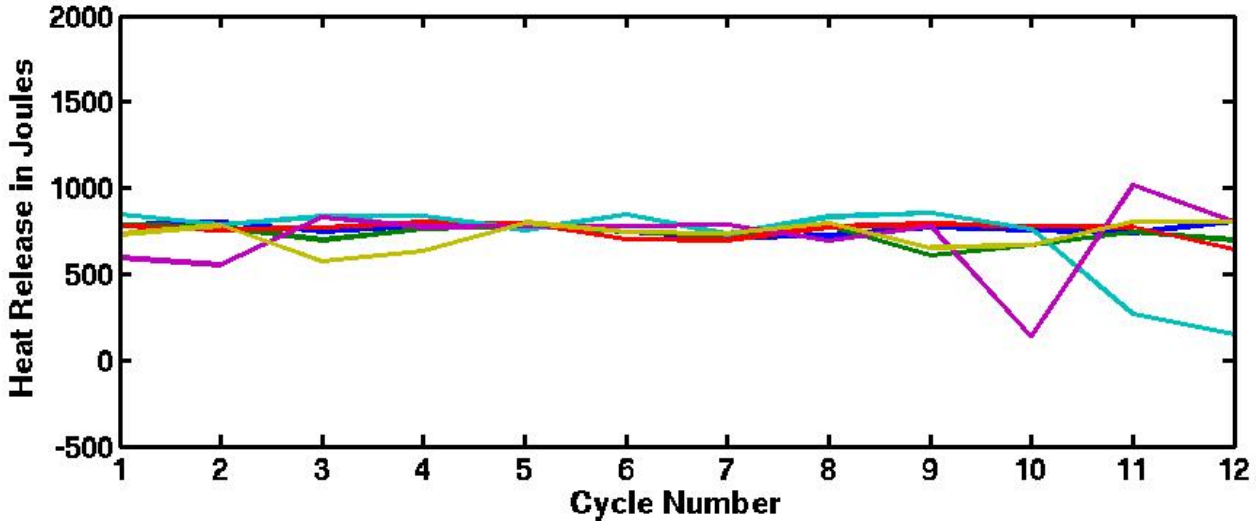
Heat Release in Joules
2000
1500
1000
500
0
-500
1
2
3
4
5
6
7
8
9
10
11
12
Cycle Number

c)

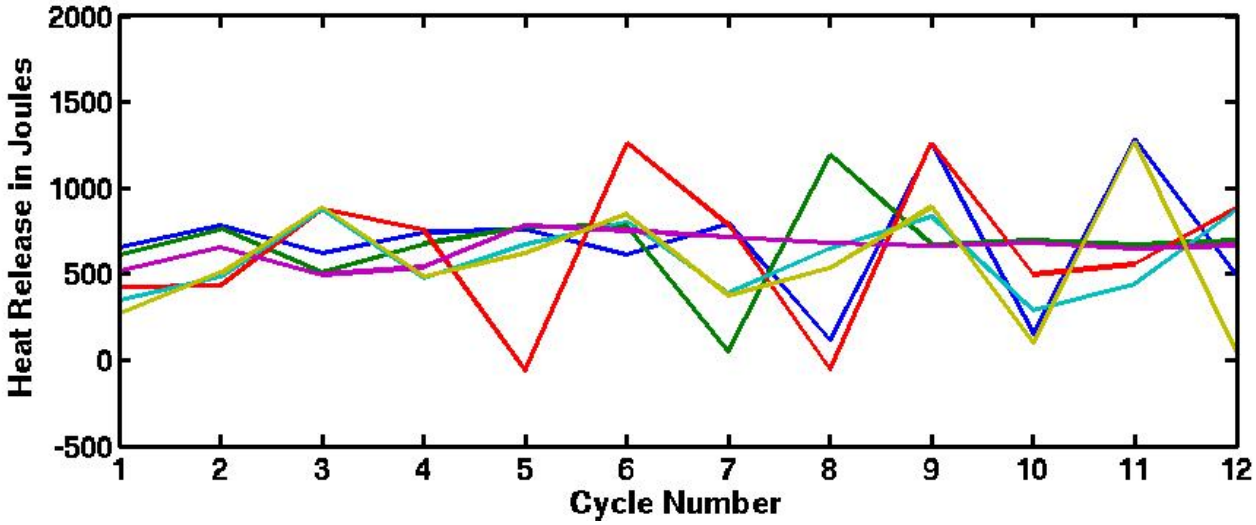
Heat Release in Joules
2000
1500
1000
500
0
-500
1
2
3
4
5
6
7
8
9
10
11
12
Cycle Number

d)

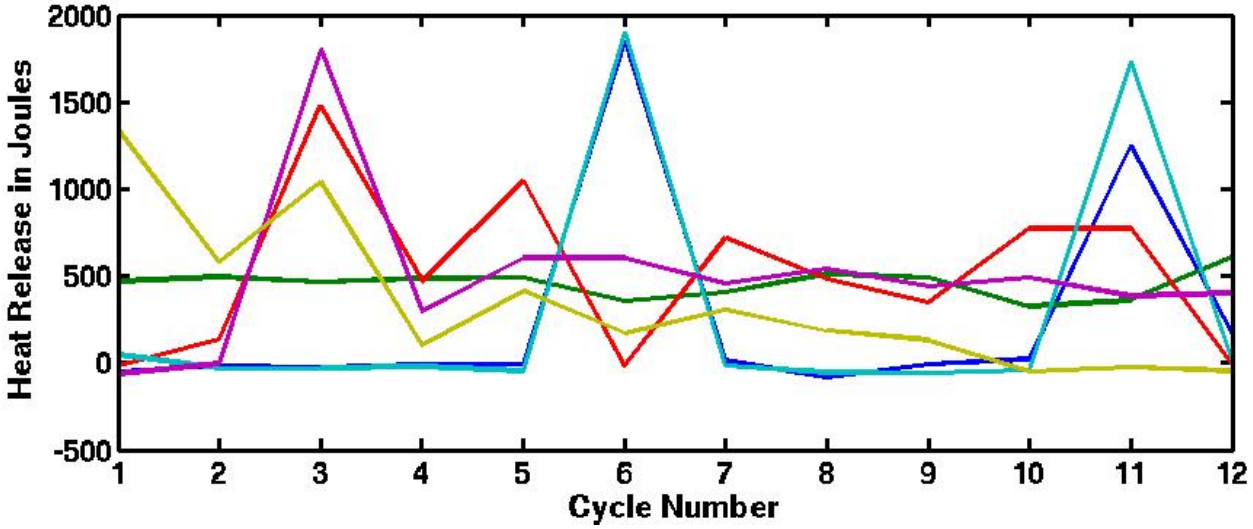

e)

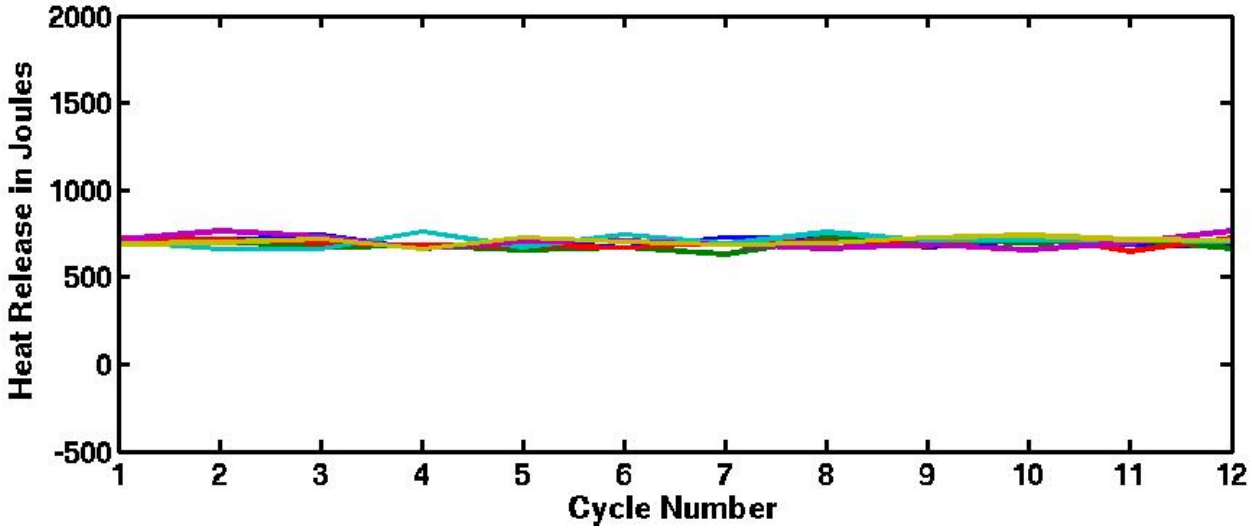

f)

Figure 2 Selected time-series segments demonstrating typical combustion behavior during steady-state operation along the SI-HCCI transition pathway. Plots a) - f) correspond to cases A-F in Table 2.

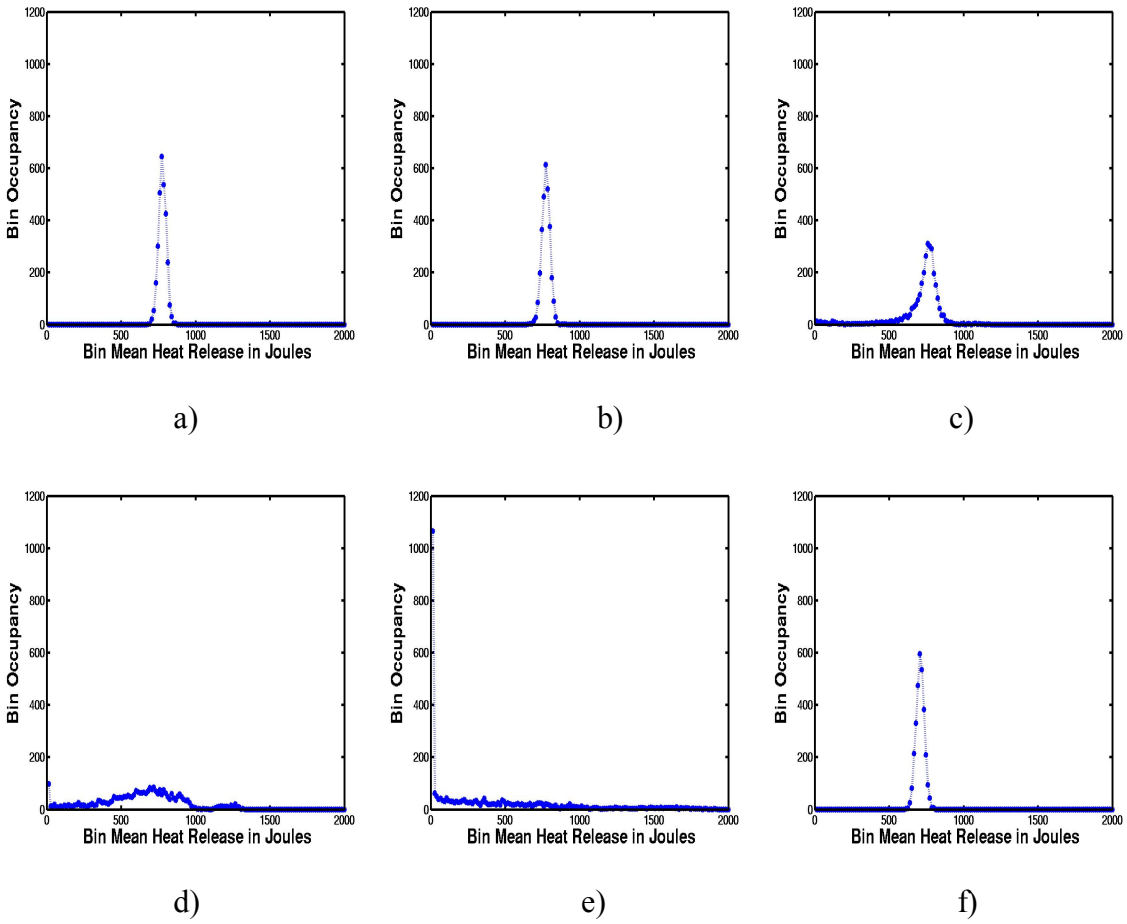

Figure 3 Histograms of cycle-integrated heat release values during steady-state operation along the SI-HCCI transition pathway. Plots a) - f) correspond to cases A-F in Table 2.

MODEL BACKGROUND

Simulation of internal combustion engines (ICE) dates to the early days of numerical computation where automated methods were first possible but spatially resolved flow fields were not. A physically detailed but spatially unresolved method was reported by Assanis and Heywood in 1986 [20]. Mass and energy balances, gas exchange, heat loss to walls and simplified combustion were combined in a model focused on diesel engine operation with turbocharger and intercooler. Andreatta [21], Aceves et.al. [22] and Easley, Agarwal and Lavoie [23] have described simplified engine models that have been heavily used. These coarsely discretized ICE models are useful if fluid mechanics effects are not dominant during the power stroke, as is the case in HCCI operation where the fuel and air are well-mixed and combustion occurs nearly simultaneously throughout the cylinder. When simple adjustments are added to compensate for phenomena in crevice zones, these models do well. Recently Verhelst and Sierens have described similar modeling and compared turbulent burning velocity models [24]. Other coarsely discretized simulations are given by Komninos et al. for HCCI combustion of iso-octane [25,26]. Reported agreement between experiment and models has been good.

Shaver et al. developed an effective simplified model for both the combustion and gas exchange portions of the ICE cycles that has utility in a controls context [27]. The gas exchange used one-dimensional gas dynamics relations and considered mass and energy balances on the exhaust manifold as well as the cylinder itself. An

integrated Arrhenius threshold was used to model combustion. This model has been widely reused and referenced [28] and has demonstrated good agreement with experimental observations for propane combustion.

Daw et al. reported SI-HCCI transition experiments for indolene combustion in the same 0.5-L research engine used here [14]. Although no physical model simulation results were presented in this experimental work, data-based models were detailed and related to physics-based models for lean-limit unstable combustion in SI engines. The data-based models involved regressive fitting of experimental heat-release estimates to obtain mapping functions from one cycle to the next [14,15,17]. With these mapping functions, noisy, experimental heat-release maps could be cleaned up to reveal the underlying dynamics in deterministic cycle-to-cycle variations.

Deterministic relations for cycle-to-cycle dynamics in spark-ignition engines had been explored in earlier work with the development of physics-based mapping functions [29-31]. The integrated-map model related masses of air and fuel, lumped on a cycle basis, with feedback from cycle to cycle via the cylinder residual gases. This model accurately described the transition from noisy stochastic dynamics at near stoichiometric fueling to noisy, chaotic dynamics at leaner fuelings, partly by using a combustion efficiency relation with nonlinear dependence on equivalence ratio, as has been observed experimentally with high-EGR transitions [32,33].

This lumped, iterated-map approach has been extended to spark-assisted HCCI combustion [16]. The model combines diluent-limited flame propagation (SI) and temperature-dependent, residual-gas driven combustion (HCCI) to compute a combustion extent and integrated heat release for each cycle. Although these mapped models can approximate the global dynamics of the combustion oscillations, they do not employ any chemical-kinetic relations in their solution.

MODEL DETAILS

During the compression and expansion portions of computed cycles, conservation relations for species, energy and mass are enforced on each of the defined in-cylinder zones. Conservation of energy on an arbitrary zone when all cylinder valves are closed is given by:

$$\frac{dT_r}{dt} = \frac{1}{\bar{c}_{p,r} m_r} \sum_{d=1}^{Z} \dot{m}_{in,d,r} \left[\sum_{i=1}^{F} (h_{d,i} - h_{r,i}) y_{d,i} \right] - \sum_{i=1}^{F} \frac{g_{r,i} h_{r,i} M_i}{\rho_r \bar{c}_{p,r}} - \frac{\dot{Q}_{loss,r}}{\bar{c}_{p,r} m_r} + \frac{1}{\rho_r \bar{c}_{p,r}} \frac{dp}{dt}. \quad (1)$$

Heat loss from zones to all solid boundaries is folded into a single term dependent on cylinder pressure and zone temperature using the power law dependence given by Woschni [34]:

$$\dot{Q}_{loss,r} = h_{woschni,r} K_r A_{total} \frac{m_r}{m_c} (T_r - T_{wall}), \quad h_{woschni,r} = k_{woschni} \left(\frac{p^{0.8}}{T_r^{0.55}} \right). \quad (2)$$

Compression work and heat generation due to chemical reaction are treated according to the manner described in [21,22]. Mass transport between zones is simplified by use of a relaxation factor, τ:

$$\dot{m}_{ex,r} = \frac{m_{r+1,init}}{\tau}. \quad (3)$$

Conservation of mass is written as

$$\frac{dm_r}{dt} = \sum_{d=1}^{z} \left(\dot{m}_{in,d,r} - \dot{m}_{ex,d,r} \right) \tag{4}$$

and the conservation of species is written as

$$\frac{dy_{r,i}}{dt} = \frac{1}{m_r} \sum_{d=1}^{z} \dot{m}_{in,d,r} \left(y_{d,i} - y_{r,i} \right) + \frac{s_{r,i} M_i}{\rho_r} . \tag{5}$$

During the exhaust and intake portions of the computed cycles, a single zone describes the in-cylinder charge and a second zone describes the exhaust manifold charge. Since we are trying to capture transient thermal and kinetic effects, particularly with regard to exhaust gas recirculation we focus on the exhaust manifold and do not similarly model the cooler, probably simpler intake side. If the intake and/or exhaust valves are open, quasi-steady one-dimensional gas dynamics relations are used to compute the mass flows according to

$$\dot{m} = \frac{C_D A p_o}{\sqrt{R T_o}} \left(\frac{p_T}{p_o} \right)^{\frac{1}{\gamma}} \left\{ \left[\frac{2\gamma}{\gamma - 1} \right] \left\{ 1 - \left[\frac{p_T}{p_o} \right]^{\frac{\gamma - 1}{\gamma}} \right\} \right\}^{1/2} \tag{6}$$

for unchoked flow or

$$\dot{m} = \frac{C_D A p_o}{\sqrt{R T_o}} \sqrt{\gamma} \left[\frac{2}{\gamma + 1} \right]^{\frac{\gamma + 1}{2(\gamma - 1)}} \tag{7}$$

for choked flow. The cylinder volume rate equation is used:

$$\dot{V} = \frac{\pi}{4} B^2 a \dot{\theta} \sin\theta \left(1 + a \frac{\cos\theta}{\sqrt{(L^2 - a^2 \sin^2\theta)}} \right) \tag{8}$$

The exhaust manifold retains a minimum mass during compression and burn so that conservation of mass in the manifold is simply:

$$\dot{m}_e = \begin{cases} 0. & : \quad -180.^\circ < \theta < EVO \\ -\dot{m}_{ec} \text{ or } \dot{m}_{ce} & : \quad EVO < \theta < EVC \\ \frac{m_{e,EVC} - m_{resid}}{EVO - EVC} \dot{\theta} & : \quad EVC < \theta < 540.^\circ \end{cases} \tag{9}$$

Thus manifold mass is held to a constant user specified value (m_{resid}) from -180° to EVO and is estimated from exhaust manifold volume, atmospheric pressure and minimum manifold gas temperature. Conservation of

energy on the manifold considers the enthalpy flows through valves, heat loss to the surroundings and expansion work done by the changing manifold volume:

$$\frac{d(m_e u_e)}{dt} = \dot{Q}_e - \dot{W}_e + \dot{m}_{ce} h_c - \dot{m}_{ec} h_e. \tag{10}$$

More specifics on this derivation are given in Shaver [28]. Species do not evolve in the exhaust manifold. When the exhaust valve closes, the mole fractions in the manifold are set to the current cylinder species mole fractions and are fixed until the next exhaust valve closing. The exhaust manifold total surface area is estimated for the heat loss model:

$$\dot{Q}_e = -h_{woschni,e} A_e (T_e - T_{surr}). \tag{11}$$

An alternate form of conservation of energy for the cylinder is used during the exhaust and intake portions of the cycle:

$$\frac{dT_c}{dt} = \frac{\frac{Q_c}{V} - (\sum_{i=1}^{F} (\dot{X}_i) \bar{h}_{c,i}) - \frac{V_c \sum_{i=1}^{F} (\dot{X}_i) \bar{h}_{c,i}}{V} + \frac{p \sum_{i=1}^{F} \dot{X}_i}{\sum_{i=1}^{F} X_i} + \frac{\sum_{valve\ flows} (\dot{m} h)}{V}}{\sum_{i=1}^{F} X_i \bar{c}_{p,i}(T) - \frac{p}{T}} \tag{12}$$

Species in the cylinder evolve or react during exhaust and intake portions of the cycle with the same kinetic rates governing but a single-zone treatment here reduces the size of the system to solve so that negligible computation time is used compared to the compress and burn portions.

$$\dot{X}_i = g_i - \frac{\dot{V} N_i}{V^2}. \tag{13}$$

Observation of diverse results from SI and HCCI simulations of compression and combustion indicates that temperature gradients from zone to zone are usually less than 20 degrees by the end of burn so that collapsing the in-cylinder model to a single zone for the gas exchange portions of the cycle probably introduces little error while greatly speeding the calculations.

This formulation does not specifically include terms for mixed mode (both flame propagation and HCCI combustion) cylinder conditions or marginal flame propagation in high EGR spark ignited combustion. As a first step in ongoing efforts to treat transitioning between modes, we have combined the mixing time constant approach (good for low EGR flame propagation and high EGR HCCI) with the aspiration and exhaust manifold modeling noted above. This is a logical first step in the overall effort. Development of mixed mode combustion relationships should follow if the current form does not adequately capture the nuances in the experimental data.

The model as described above produces pressure histories during single compression and expansion strokes which agree well with experimental measurements for motored operation, typical SI (EGR~10%) and HCCI combustion (EGR~75%) as shown in Figure 4. . We expect that the model has sufficient physical detail to capture the qualitative trends of the SI to HCCI transition process.

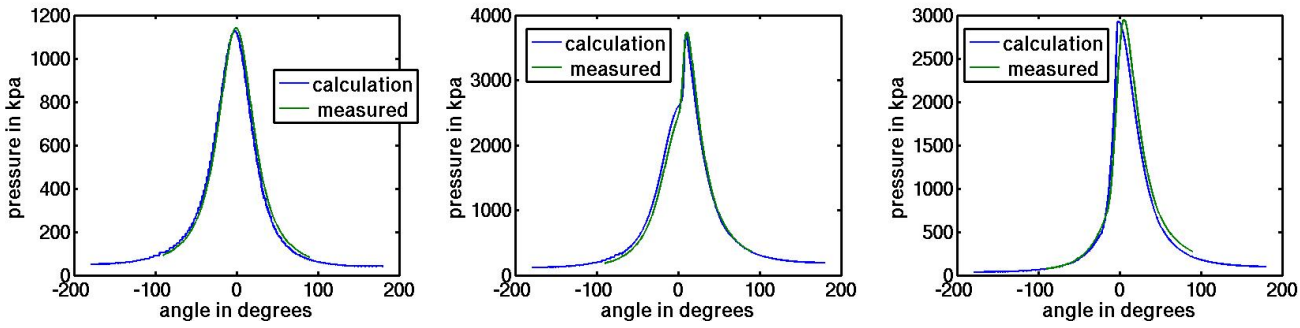

Figure 4 Comparison of experimental and simulated cylinder pressure profiles for a) motored mode, b) spark-ignited mode and c) HCCI mode.

MODEL DEVELOPMENT

We describe here the progressive development of our model for the SI-HCCI transition described in the previous section. Our approach involved incrementally adding detail to improve agreement between the model and experimental observations. Iso-octane is an excellent choice for this transition focused study because we have extensive experience with using moderately simplified kinetic mechanisms for it which yield good comparison to test [35].

As a first approximation, only the compression and expansion strokes were modeled (see equations 1 to 5). Successive cycles were modeled as follows: a portion of the residual gases from the previous cycle was mixed with a stoichiometric mixture of fresh air and fuel to obtain the desired EGR level. This mix was given an initial post-mixing temperature and combustion was simulated during the compression and expansion strokes (-180° to +180° ATDC). This process was repeated for 10 to 20 successive cycles. Simulations were performed for a matrix of EGR and initial post-mixing temperatures to determine if variations in the initial energy content and kinetic peculiarities of the unburned fuel and fuel fragments were sufficient to cause the cycle-to-cycle variability observed experimentally. This approach only yielded successive full burns or simply oscillating complete burns and incomplete burns of low magnitude.

We next added stochastic perturbations to the EGR level, average cylinder temperature, zone-to-zone temperature, and intake pressure. These perturbations were intended as physically reasonable representations of the tendency of misfiring cylinders to have disrupted flow patterns. For example, scavenging of burned vs. unburned gases may vary randomly from cycle to cycle depending on their relative location within the cylinder at exhaust valve opening. Other phenomena such as standing acoustic waves in the intake and exhaust manifolds and other non-idealities may also contribute to complex combustion oscillations. While the addition of stochastic perturbations to the above parameters did create more cycle-to-cycle variability, the predicted variations were still far less rich than those observed experimentally. On the other hand, such variations are similar to previously reported experimental observations and model simulations of combustion under highly dilute conditions (due to either lean fueling or high levels of EGR) [29-32].

As a next step in increasing model fidelity, we expanded the model to include the entire cycle by combining the above approach for the compression and expansion strokes (eqns. 1 to 5) with the manifold and valve treatment

(eqns. 6 to 13) as described in the theory section during the exhaust and intake strokes. Stochastic perturbations were added to the discharge coefficients of both valves to account for:

1) Poor or badly timed burns resulting in off-normal, dissipative and highly non-ideal gas exchange typified by transient shocks and in some cases flows in undesired directions.

2) Inhibited mixing processes between clean intake and retained or re-inducted combustion products.

3) Poor burns resulting in significant heat release in the exhaust system, which then disturbs normal flow.

Thus for each of the six cases A through F, we have tried a range of discharge coefficients strongly influenced by the values measured by the engine manufacturer for the valves. We have also used a range of stochastic variation on these discharge coefficients from cycle to cycle, as given in Table 3. Note that the discharge coefficient used in the model represents a sum of the flow dissipative effects of the entire flow passage (intake or exhaust) while the manufacturer's measured value is for just the valve. For example, throttling of the intake to the engine caused the discharge coefficient used in the model for the intake system to be much lower than the discharge coefficient measured for the intake valve alone. The added complexity of the full model required the addition of a fast iterative solver for the Jacobian matrix described by McNenly et al. [12] to maintain a reasonable computational time.

Table 3 Range of discharge coefficients for intake and exhaust valves ($C_{D,i}$ and $C_{D,e}$) used in the model compared to flow-test values for the experimental engine measured at maximum lift

Case	$C_{D,i}$	$C_{D,e}$	$C_{D,i}$ measured	$C_{D,e}$ measured	Number of simulated cycles
A	0.190 - 0.192	0.4528 - 0.4532	0.403	0.453	100
B	0.205 - 0.235	0.3645 - 0.4245	0.405	0.425	100
C	0.05 - 0.30	0.16 - 0.51	0.405	0.410	100
D	0.14 - 0.30	0.3800 - 0.4245	0.407	0.394	100
E	0.20 - 0.26	0.34 - 0.38	0.409	0.356	500
F	0.330 - 0.331	0.360 - 0.361	0.412	0.316	500

While not a first principle-based solution, the method is computationally efficient and a useful first approach to the problem. More physically representative solutions (such as KIVA-based 3-dimensional modeling of transient intake and exhaust flows coupled to the reacting cylinder flow field) demand extreme computational resources for multiple-cycle analysis and are therefore impractical at this time. Cycle-to-cycle dynamics computed by the simulation are presented in Figures 5 and 6 for comparison to the corresponding experimental results in Figures 2 and 3.

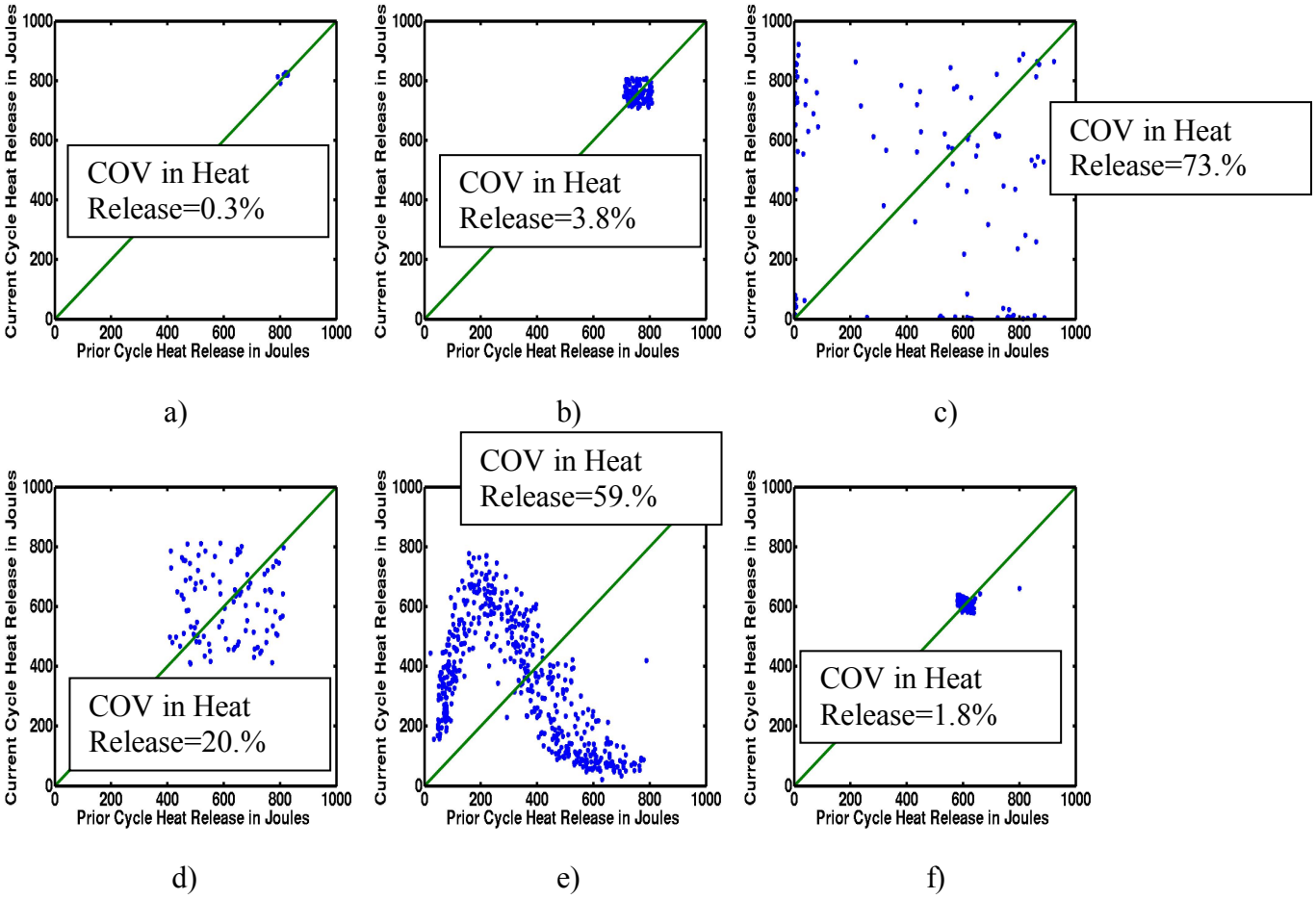

Figure 5 Heat release return maps from simulation. Plots a) - f) correspond to cases A-F in Table 2.

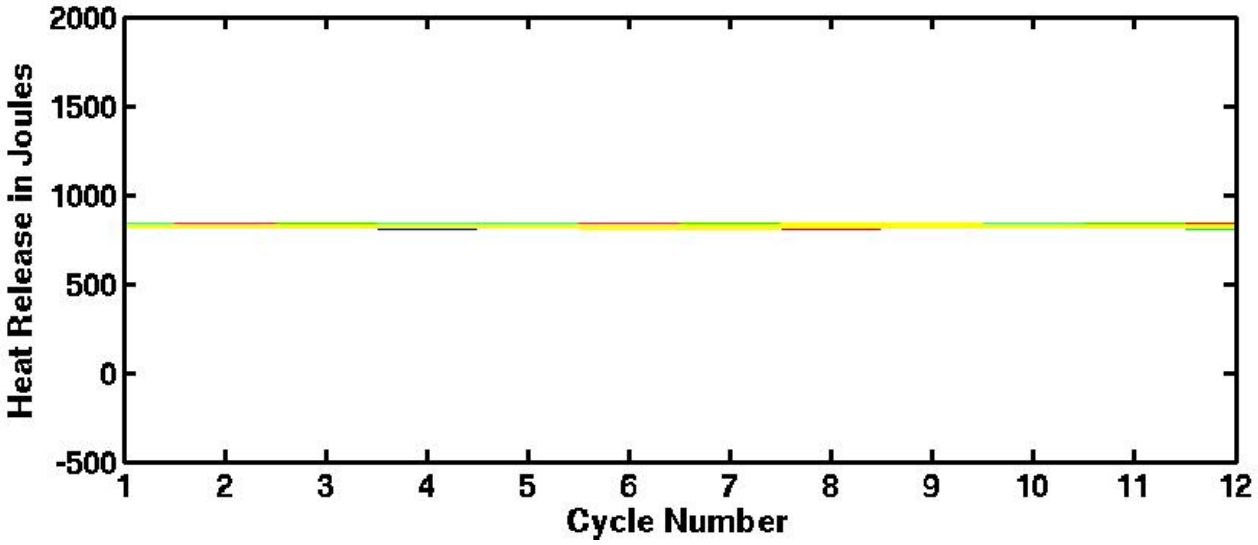

a)

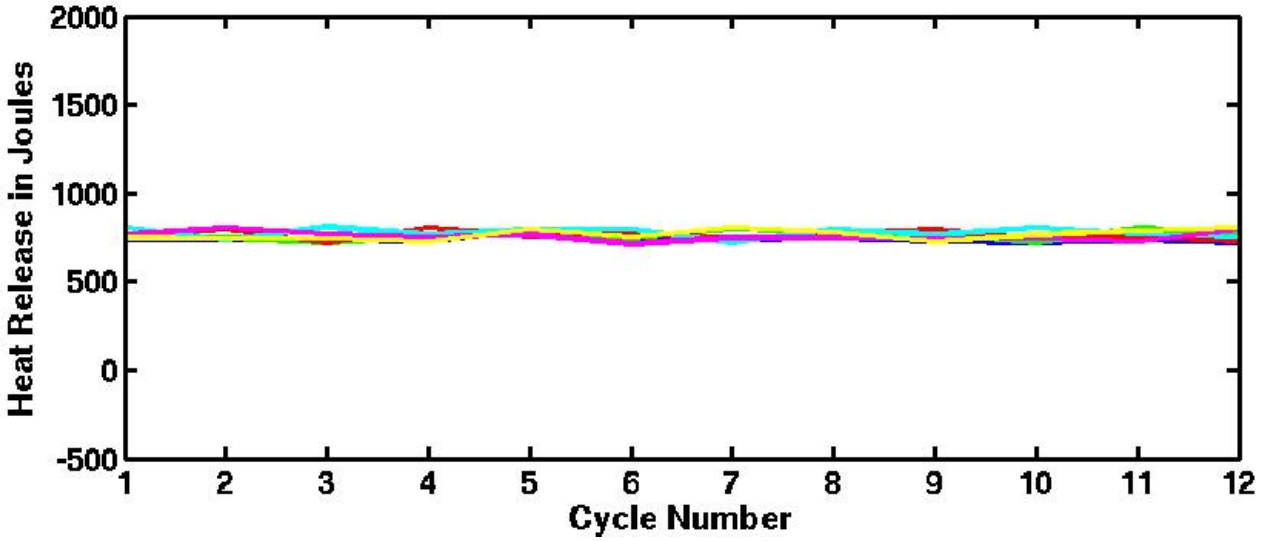
Heat Release in Joules
2000
1500
1000
500
0
-500
1
2
3
4
5
6
7
8
9
10
11
12
Cycle Number

b)

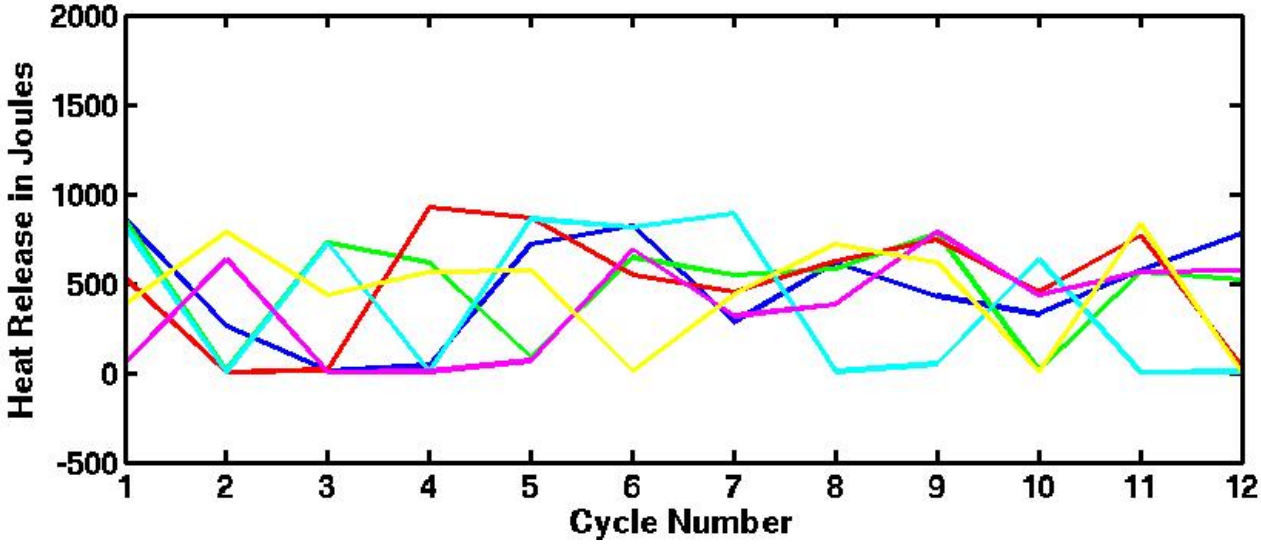
Heat Release in Joules
2000
1500
1000
500
0
-500
1
2
3
4
5
6
7
8
9
10
11
12
Cycle Number

c)

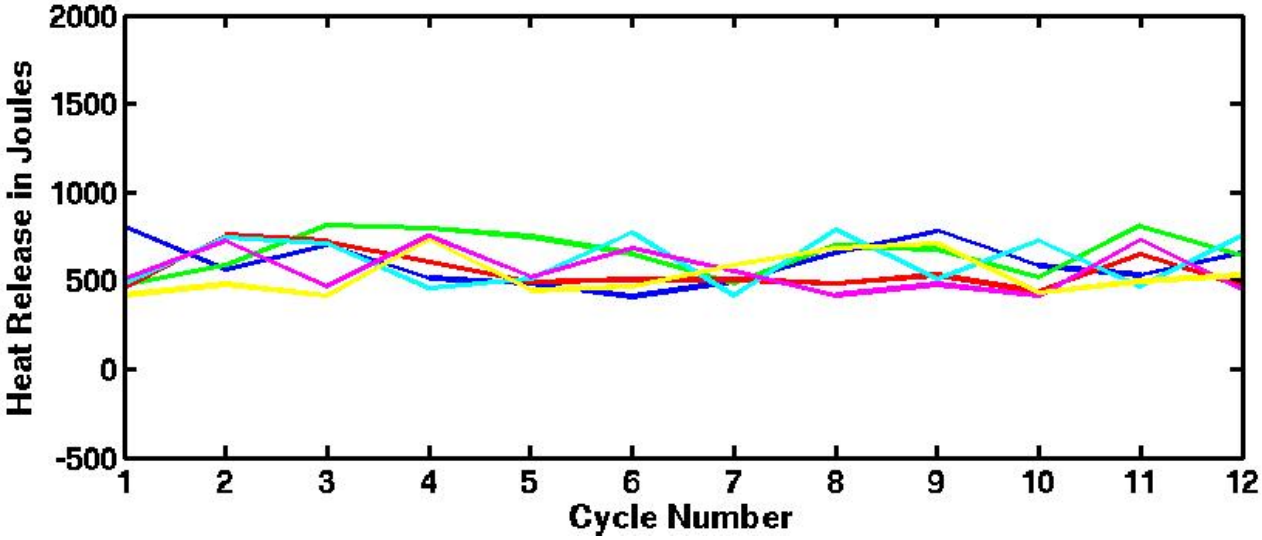
Heat Release in Joules
2000
1500
1000
500
0
-500
1
2
3
4
5
6
7
8
9
10
11
12
Cycle Number

d)

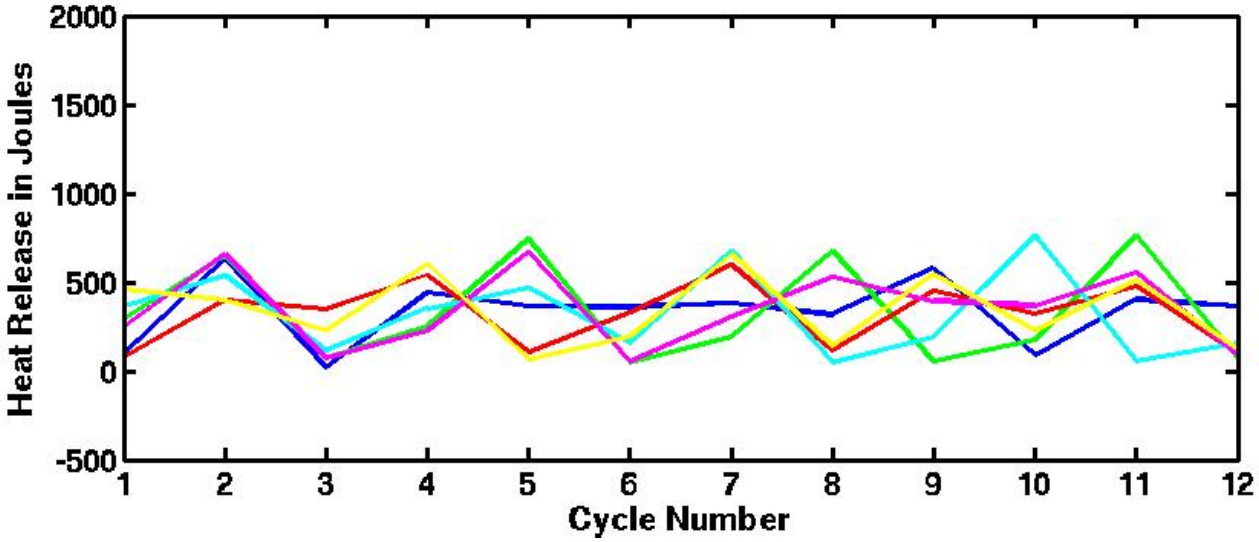
Heat Release in Joules
2000
1500
1000
500
0
-500
1
2
3
4
5
6
7
8
9
10
11
12
Cycle Number

e)

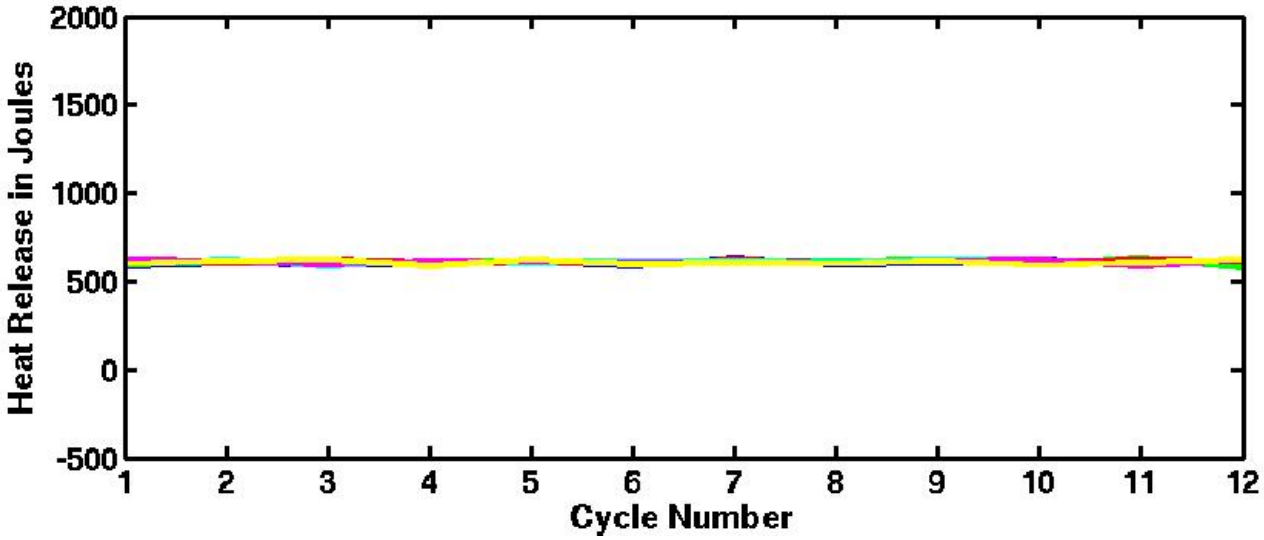

f)

Figure 6 Sequential heat release from simulation. Plots a) - f) correspond to cases A-F in Table 2.

The current model appears to capture the global behavior of the SI-HCCI transition with stable SI and HCCI combustion and very unstable behavior during the transition. However, upon closer inspection, much of the complex, underlying dynamics observed experimentally are missing or under-represented in the model results. As discussed above, instabilities in the experimental system typically follow a three-step pattern with two cycles of incomplete combustion (SI followed by HCCI) with relatively low heat releases followed by a robust spark-assisted HCCI event with a relatively high heat release. While a similar pattern can be observed in the simulation results (especially in Figures 6c and e), the instabilities in the model appear to be dominated by a two-step misfire and recovery pattern. This results in the boomerang-shaped return map shown in Figure 5e (and suggested in Figure 5c) which is more typical of very dilute SI combustion [29-32] and is distinctly different than the more complex behavior seen experimentally. This perhaps suggests that the model is accurately representing the effects of dilution on SI combustion but not fully capturing the effects of spark-assist on HCCI at these intermediate-residual cases. Another aspect of the experimental observations not captured by the model is the frequent successive misfires and engine stall observed in case E. The current model assumes a constant cylinder wall temperature and thus does not capture engine cool-down caused by successive misfires. There are reasons for optimism though as there is evidence of short-term stability at these intermediate conditions (as indicated by example time series segments in Figures 6c-e showing several successive cycles with limited variability in heat release).

CONCLUSIONS

We have described a first step in applying a multi-zone chemical kinetic model for simulating the dynamics of the SI-HCCI transition and spark-assisted HCCI. The model attempts to provide a balance between the numerical complexity of multidimensional CFD modeling – computationally expensive for running multiple consecutive cycles necessary for transition modeling – and the extreme simplicity of zero-dimensional lumped models based on burn duration correlations that may not capture complex transient phenomena. The present

multi-zone model requires tuning of the mass exchange between zones and stochastic variability of the discharge coefficient.

The model has been shown to predict unstable combustion at intermediate points along the transition pathway between stable SI and HCCI combustion (even in the absence of stochastic perturbations). While the predicted behavior appears more similar to observations of highly dilute SI combustion, there are indications that the model predicts the more complex behavior observed experimentally. Thus, while the model does capture the overall pattern of instability during the SI-HCCI transition, it appears more work is needed to fully capture the complex dynamics driving the instabilities. This information is crucial to the development of efficient control strategies to smooth the transition and promote stable spark-assisted HCCI operation. The model may be upgraded by incorporating a more detailed fluid mechanical treatment of the aspiration phenomena. Wave effects in the intake and exhaust flows may be required to better simulate experiment. Probably of greater significance would be an upgrade to quantify temporally and spatially mixed HCCI and flame propagation combustion. This is computationally complex but may be required to fully capture experimental dynamics. Successful development of this aspect of the model would facilitate modeling of mode transitions and comparison to work at higher loads.

DEFINITIONS/ABBREVIATIONS

A area

a half the stroke length

B bore diameter

C_D discharge coefficient

c_p specific heat at constant pressure

COV coefficient of variation

EVC exhaust valve closing

EVO exhaust valve opening

F number of species

g species production rate

h enthalpy or convection coefficient depending on context

IVC intake valve closing

IVO intake valve opening

K multiplier on Woschni heat transfer

k correlation constant in Woschni relation

L connecting rod length

M molecular weight

m mass

N moles

p pressure

Q heat flow rate

R gas constant

T temperature

t time

u internal energy

V volume

W work

X molar concentration

y mass fraction

Z number of reactors in cylinder discretization

γ ratio of specific heats

ρ density

τ relaxation time constant

θ angular position of piston in cylinder

Subscripts and other notations

c cylinder conditions

ce cylinder to exhaust condition

conv convection

e exhaust valve or exhaust manifold conditions

ec exhaust to cylinder conditions

ex exit flow

i species index

in inlet conditions

init initial

loss heat flow to surroundings from working fluid

o stagnation conditions

r reactor index

resid minimum mass condition in exhaust manifold

surfs wall plus head plus piston

surr conditions for exhaust manifold surroundings

T total conditions

wall "wall" in reactor model combines wall, piston and head

^ molar basis

- averaged over mass fractions

REFERENCES

1. Weinrotter, M., Iskra, K., Wintner, E., Neger, T., Olofsson, J., Alden, M., Seyfried, H., Lackner, M., Winter, F., Hultqvist, A., Vressner, A., Johansson, B., "Optical diagnostics of laser-induced and spark plug-assisted HCCI combustion", SAE 2005-01-0129, 2005.
2. Urushihara, T., Yamaguchi. K., Yoshizawa, K., Itoh, T., "A study of a gasoline-fueled compression ignition engine – expansion of HCCI operation range using SI combustion as a trigger of compression ignition", SAE paper 2005-01-0180, 2005.
3. Santoso, H.G., Matthews, J., Cheng, W.K., "Managing SI/HCCI dual-mode engine operation", SAE paper 2005-01-0162, 2005.
4. Hyvonen, J., Johansson, B., "Operating conditions using spark assisted HCCI combustion during combustion mode transfer to SI in a multi-cylinder VCR-HCCI engine", SAE paper 2005-01-0109, 2005.

5. Koopmans, L., Denbratt, I., Backlund, O., ”Cycle-to-cycle variations: their influence on cycle resolved gas temperature and unburned hydrocarbons from a camless gasoline compression ignition engine”, SAE paper 2002-01-0110, 2002.
6. Daw, C.S., Edwards, K.D., Wagner, R.M., Green, J.B. Jr., “Modeling cyclic variability in spark-assisted HCCI”, ASME Journal of Engineering for Gas Turbines and Power, 130:052801, 2008.
7. Yasar, H., Soyhan, H.S., Walmsley, H., Head, B., Sorusbay, C., “Double-Wiebe function: an approach for single-zone HCCI engine modeling”, Applied Thermal Engineering, Vol. 28, pp. 1284-1290, 2008.
8. Ra, Y., Reitz, R.D., “A reduced chemical kinetic model for IC engine combustion simulations with primary reference fuels”, Combustion and Flame, Vol. 155, pp. 713-738, 2008.
9. Curran, H.J., Gaffuri, P., Pitz, W.J., Westbrook, C.K., “A comprehensive modeling study of iso-octane oxidation,” Combustion and Flame, Vol. 129, pp. 253-280, 2002.
10. Amsden, A.A., “KIVA-3V, Release 2, Improvements to KIVA-3V,” Los Alamos National Laboratory, LA-UR-99-9154, 1999.
11. Chen, J.-Y., Tham, Y.F., “Speedy solution of quasi-steady-state species by combination of fixed-point iteration and matrix inversion”, Combustion and Flame, Vol. 153, pp.634-646, 2008.
12. McNenly, M.J., Havstad, M.A., Aceves, S.M., Pitz, W.J., "Preconditioning Strategies for Efficient Multizone Chemical Kinetic Models," SAE conference paper 10PFL-0862, SAE World Congress 2010, spring 2010.
13. Heywood, J.B., Internal Combustion Engine Fundamentals, New York, McGraw-Hill, ISBN 007028637X, 1988.
14. Wagner, R.M., Edwards, K.D., Daw, C.S., Green, J.B., Bunting, B.G., “On the nature of cyclic dispersion in spark assisted HCCI combustion,” SAE paper 2006-01-0418, 2006.
15. Daw, C.S., Wagner, R.M., Edwards, K.D., Green, J.B. Jr., “Understanding the transition between conventional spark-ignited combustion and HCCI in a gasoline engine”, Proceedings of the Combustion Institute, Vol. 31, pp. 2887-2894, 2007.
16. Daw, C.S., Edwards, K.D., Finney C.E.A., Wagner, R.M., “A simple model for exploring the cyclic dynamics of spark-assisted HCCI”, Proceedings of the 6th US National Combustion Meeting, 2009.
17. Edwards, K.D., Wagner, R.M., Daw, C.S., Green, J.B. Jr., “Hybrid SI-HCCI combustion modes and the potential for control”, Proceedings of the 5th US National Combustion Meeting, 2007.
18. Daw, C.S., Edwards, K.D., Wagner, R.M., Green, J.B. Jr., “Modeling cyclic variability during the transition between spark-ignited combustion and HCCI”, Proceedings of the 5th US National Combustion Meeting, 2007.
19. Glewen, W.J., Wagner, R.M., Edwards, K.D., Daw, C.S., “Analysis of cyclic variability in spark-assisted HCCI combustion using a double Wiebe function”, Proceedings of the Combustion Institute, Vol. 32, pp. 2885-2982, 2009.
20. Assanis, D.N., Heywood, J.B., “Development and use of a computer simulation of the turbocompounded diesel system for engine performance and component heat transfer studies,” SAE paper 860329, 1986.
21. Andreatta, D.A., “The use of reformed natural gas as a fuel for reciprocating engines”, Ph.D. dissertation, University of California at Berkeley, Dept. of Mechanical Engineering, 1995.
22. Aceves, S.M., Flowers, D.L., Westbrook, C.K., Smith, J.R., Dibble, R.W., Christensen, M., Pitz, W.J., Johansson, B., “A multi-zone model for prediction of HCCI combustion and emissions”, SAE paper 2000-01-0327, 2000.
23. Easley, W.L., Agarwal, A., Lavoie, G.A., “Modeling of HCCI combustion and emissions using detailed chemistry,” SAE paper 2001-01-1029, 2001.
24. Verhelst, S., Sierens, R., “A quasi-dimensional model for the power cycle of a hydrogen-fuelled ICE”, International Journal of Hydrogen Energy, Vol. 32, pp. 3545-3554, 2007.

25. Komninos, N.P., Hountalas, D.T., “Improvement and validation of a multi-zone model for HCCI engine combustion concerning performance and emissions”, Energy Conversion and Management, Vol. 49, pp. 2530-2537, 2008.
26. Komninos, N.P., Hountalas, D.T., Kouremenos, D.A., “Description of in-cylinder combustion processes in HCCI engines using a multi-zone model”, SAE paper 2005-01-0171, 2005.
27. Shaver, G.M., Roelle, M.J., Gerdes, J.C., “Modeling cycle-to-cycle dynamics and mode transition in HCCI engines with variable valve actuation,” Control Engineering Practice, Vol. 14, pp. 213-222, 2006.
28. Bengstton, J., Gafvert, M., Strandh, P., "Modeling of HCCI Engine Combustion for Control Analysis," 43rd IEEE Conference on Decision and Control, Dec. 14-17, 2004, Paradise Island, Bahamas.
29. Daw, C.S., Finney, C.E.A., Green, J.B. Jr., Kennel, M.B., Thomas, J.F., Connolly, F.T., “A simple model for cyclic variations in a spark-ignition engine”, SAE paper 962086, 1996.
30. Daw, C.S., Kennel, M.B., Finney, C.E.A., Connolly, F.T. “Observing and modeling nonlinear dynamics in an internal combustion engine”, Physical Review E, Vol. 57, pp. 2811-2819, 1998.
31. Wagner, R.M., Daw, C.S., Green, J.B. Jr, “Low-order map approximations of lean cyclic dispersion in premixed spark ignition engines”, SAE paper 2001-01-3559, 2001.
32. Sutton, R.W., “Investigation of cyclic dispersion under lean fueling and high levels of simulated EGR”, M.S. thesis, University of Missouri - Rolla, 2000.
33. Shyani, R.G., Caton, J.A., “A thermodynamic analysis of the use of exhaust gas recirculation in spark ignition engines including the second law of thermodynamics”, Journal of Automobile Engineering, Vol. 223, pp. 131-149, 2009.
34. Woschni, G., “A universally applicable equation for the instantaneous heat transfer coefficient in the internal combustion engine”, SAE paper 670931, 1967.
35. Aceves, S.M., Martinez-Frias, J., Flowers, D.L., Smith, J.R., Dibble, R.W., Wright, J.F., C.K., Hessel, R.P., “A Decoupled Model of Detailed Fluid Mechanics Followed by Detailed Chemical Kinetics for Prediction of Iso-Octane combustion”, SAE paper 2001-01-3612, 2001.

CONTACT INFORMATION

For questions or comments contact Mark A. Havstad, havstad1@llnl.gov.

ACKNOWLEDGMENTS

This project is funded by DOE, Office of Vehicle Technologies, Gurpreet Singh and Kevin Stork, program managers. This work performed under the auspices of the U.S. Department of Energy by Lawrence Livermore National Laboratory under Contract DE-AC52-07NA27344.